JOURNAL OF CATALYSIS 47, 343-357 (1977)

The Catalytic Cracking of Cumene

The Kinetics of the Dealkylation Reaction

DONALD A. BEST[1] AND BOHDAN W. WOJCIECHOWSKI[2]

Department of Chemical Engineering, Queen's University, Kingston, Ontario, Canada

Received February 23, 1976; revised January 21, 1977

In a previous paper [*J. Catal.* **31**, 74 (1973)] the Campbell–Wojciechowski mechanism for cumene cracking was applied to cumene conversion data obtained on various mesh sizes of LaY catalyst in order to study the effects of diffusion on the model parameters. Here, the diffusion free region is isolated and the intrinsic kinetics are determined. The activation energy for the dealkylation reaction is found to be 22.5 kcal/mole, which is in good agreement with results reported by other workers. Furthermore, when this value of activation energy is used in an analysis of the energetics of the reaction, it is shown that endothermic chemisorption of cumene must be assumed in order to construct a plausible picture of the reaction energy surface.

It is also shown that diffusion limitations affect the rate of catalyst decay to a different extent than they affect the rate of reaction. This confirms our belief that the standard experimental procedure to test the significance of intraparticle diffusion must be modified in a manner suggested in a previous publication [*Canad. J. Chem. Eng.* **54**, 197 (1976)] in order to avoid misinterpreting the results of diffusion studies on decaying catalysts.

NOMENCLATURE

b	proportionality constant relating space time τ to cat/oil ratio P and final catalyst time on stream t_f; $\tau = bPt_f$
c	symbol representing cumene
E	energy of adsorption, cal/mole
E_2	activation energy for rate constant k_2, cal/mole
G	aging parameter defined by Eq. (22)
H	enthalpy, cal/mole
k	rate constant for cumene cracking
k_d	proportionality constant including a rate constant for deactivation
K	adsorption equilibrium constant, atm^{-1}
N	aging parameter defined by Eq. (21)
p, q, s	cumene cracking model parameters, dimensionless
p', q', s'	modified model parameters, sec.
P	cat/oil ratio defined as the weight of catalyst to weight of reactant
$[P]$	concentration of poison species
t_f	final catalyst time on stream, sec.
t	instantaneous catalyst time on stream
$\bar{x}$	average conversion of cumene
x	instantaneous conversion of cumene
x_e	equilibrium conversion of cumene
Y	component of the delta mechanism, represents propylene
Z	component of the delta mechanism, represents benzene

[1] Research Department, Imperial Oil Enterprises Ltd., Sarnia, Ontario.

[2] To whom correspondence should be addressed.

ISSN 0021-9517

Subscripts

1, 2, 3, 4 steps of the Delta mechanism
- 1 adsorption/desorption of cumene[3]
- 2 alkylation/dealkylation reaction
- 3 adsorption/desorption of propylene[3]
- 4 adsorption/desorption of benzene[3]

INTRODUCTION

In an earlier paper of this series (*3*), a detailed examination of the products of this reaction was made in order to identify which of the many products are primary, which are secondary, and whether they are stable or unstable under reaction conditions. Using this information a reaction mechanism was developed. The discussion in this paper concentrates on the kinetics of the most important reaction in that mechanism: dealkylation.

METHODS

Reaction Kinetics

In most cases the mechanism of the cumene cracking reaction has been studied using one of the three common reactor types: microcatalytic, differential and integral. Of these, the most frequently used appears to be the microcatalytic and a number of examples of such works are listed in Table 1. Unfortunately, with this type of reactor several difficulties are encountered. The first is the so-called "chromatographic effect" which occurs when a reactant or product is less strongly adsorbed than other species in the reaction mixture. The consequent separation disturbs the equilibrium with the result that either complete conversion is obtained or a steady state is established away from true equilibrium. Nearly all studies using a microcatalytic reactor to crack cumene report conversions above the thermodynamic value and many indicate complete conversion at temperatures lower than 400°C, when thermodynamic equilibrium is less than 64%. Turkevich and Ono (*28*) are among the few who have noticed this anomaly. The second difficulty encountered with the microcatalytic reactor, as noted by Bassett and Habgood (*1*), is that the quantitative treatment is limited to first order reactions when the partial pressure of reactant is low and the surface reaction is rate controlling. These conditions may not be fulfilled in the case of cumene cracking.

Such difficulties do not arise when a differential reactor is used. Table 1 includes several cumene cracking studies that use this reactor type; of these the most comprehensive work is that carried out by Prater and Lago (*22*). Assuming the mechanism,

$$C + S \underset{k-1}{\overset{k_1}{\rightleftarrows}} CS \xrightarrow{k_2} \text{products},$$

they developed a rate equation of the form

$$\text{rate} = \frac{k_2[S]K_1[C]}{1 + (k_2/k_1) + K_1[C]},$$

where

- $[S]$ concentration of active sites
- $[C]$ concentration of cumene
- K_1 equilibrium adsorption constant
- $-r_c$ rate of loss of cumene.

The reaction was found to be zero order at low pressure and temperature and a transition to first order appeared to occur at higher temperatures. The effect of inhibitors was also studied in this case. Unfortunately, the rate of cracking was determined by the rate of formation of gaseous products, and Pansing and Malloy (*20*) have shown this to be an incorrect approach. These workers in turn used the rate of benzene formation to illustrate the general adequacy of the Prater–Lago mechanism. Horton and Maatman (*16*) also used benzene formation as a measure of cumene conversion but they

[3] Here adsorption and desorption are used in the sense of formation and decomposition of the activated species in the reaction.

TABLE 1

A Tabulation of Some Published Studies of the Cumene Cracking Reaction[a]

Reactor type	Catalyst	Kinetic rate expression used	Activation energy (kcal/mole)	Ref.
Microcatalytic	Decationized zeolite	$kK_1 = \frac{-F}{273RW} \ln (1 - x)$	14.5	Bezre *et al.* (*7*)
	Decationized zeolite	$kK_1 = \frac{-F}{273RW} \ln (1 - x)$	18.0	Romanovskii *et al.* (*25*)
	Alkaline and alkaline earth zeolite	$r = \frac{[S_0]k_BT}{h} \exp\left(\frac{-E}{RT}\right)$	28.2–30.0	Richardson (*23*)
	Yytrium Y LaY Amorphous SiAl	first order power law expression	17.0–24.0 17.0–18.0 15	Topchieva *et al.* (*27*)
	Decationized Y	$k = \frac{-F}{W} \ln (1 - x)$	24	Turkevich and Ono (*28*)
	Ca and NaX and Y zeolite	$k'K_1 = \frac{-F}{273W} \ln (1 - x)$	29.0–47.0	Boreskova *et al.* (*8*)
	HCl + zeolite	$r = k_2(1 - x) + k_{-2}x$		Matsumoto *et al.* (*18*)
Differential	Amorphous SiAl	$r = \frac{k_2[S_0]K_1[C]}{1 + K_1[C]}$	20.6	Pansing and Malloy (*20*)
	Amorphous SiAl	$r = \frac{k_2[S_0]K_1[C]}{1 + (k_2/k_1) + K_1[C]}$	27.7–29.5	Horton and Maatman (*16*)
	Amorphous SiAl	$r = \frac{k_2[S_0]K_1[C]}{1 + (k_2/k_1) + K_1[C]}$	40.0	Prater and Lago (*22*)
	Cogelled silica alumina	$r = \frac{k_2[S_0]K_1[C]}{1 + (k_2/k_1) + K_1[C]}$	23.6–27.0	Maatman *et al.* (*17*)
	HY CaY LaY	$r = \frac{k'K_1[C]}{1 + K_1[C]}$	34.2 29.7 26.5	Romanovskii *et al.* (*24*)
Tubular	Silica alumina	$r = \frac{k_2[S_0]K_1\{[C] - [Y][Z]/K\}}{1 + K_1[C] + K_4[Z]}$	11.1	Corrigan *et al.* (*10*)
	SmY zeolite	$k = \frac{F}{W} - \ln (1 - x)$	20.0	Eberly and Kimberly (*11*)
	LaY	$r = \frac{k_2K_1[C][S] - k_{-2}K_3[Y][Z][S]}{1 + K_1[C] + K_4[Z] + K_3[Y]}$	19.5	Campbell and Wojciechowski (*9*)
	LaY	$r = \frac{k_2K_1[C][S] - k_{-2}K_3[Y][Z][S]}{1 + K_1[C] + K_4[Z] + K_3[Y]}$	22.1	Best and Wojciechowski (*6*)
	LaY	$r = \frac{k_2K_1[C][S] - k_{-2}K_3[Y][Z][S]}{1 + K_1[C] + K_4[Z] + K_3[Y]}$	22.5	This work

[a] Additional nomenclature used in this table not listed in text: F = flow rate of carrier gas; W = weight of catalyst; k_B = Boltzmann's constant; h = Planck's constant; R = gas law constant; K = equilibrium constant for the reaction.

worked solely in the region of zero order kinetics. Previously (*3*) we have shown that benzene is not the only primary product of this reaction thus bringing into question the results of this work.

The advantages of using a differential reactor have been well documented. However, Best and Wojciechowski (*4*) have shown that if an aging catalyst is used, and if such a catalyst is pre-aged to some steady state value (which is the case with the majority of the differential studies reported in table 1) the observed activation energy and preexponential factor may not represent the true value. Another problem which arises when using a differential reactor is that the effect of the back reaction is generally neglected.

These difficulties can be avoided by using an integral reactor. Corrigan *et al.* (*10*) appear to be among the few to use this type of reactor to elucidate the mechanism of the cumene cracking reaction. Unfortunately, it was subsequently shown by

Prater and Lago (*22*) that Corrigan's data were strongly affected by diffusion. No other detailed study of cumene dealkylation using an integral reactor appeared until 1971 when Campbell and Wojciechowski (*9*) presented a comprehensive mechanism for cumene cracking which is consistent with the Prater–Lago mechanism but, unlike previous mechanisms, describes cumene cracking at all levels of conversion and accounts for catalyst aging. The resultant rate equation was successfully fitted to data obtained on a 30/60 mesh LaY, but it was later shown by Best and Wojciechowski (*6*) that in Campbell's work intraparticle diffusion was still significant at the highest temperature used.

In this work the diffusion free region is finally identified and the true kinetic parameters are obtained. In addition, the cumene cracking model is used to study diffusion limitations and to observe its effects on the reaction parameters. Although simultaneous diffusion and aging may often be present in catalytic cracking, little has been done to study both phenomena together. When the Campbell–Wojciechowski cumene cracking model is applied to data obtained at conditions involving various diffusion limitations and temperatures, an analysis of the parameters obtained allows the effect of intraparticle diffusion on the reaction rate to be separated from the aging effect and hence each effect can be studied independently.

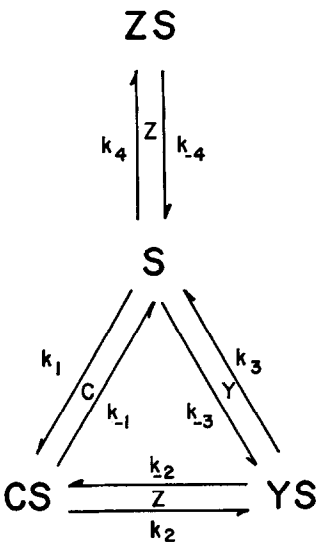

FIG. 1. The delta mechanism for the dealkylation of cumene. C represents cumene, S an active site, and Y and Z the reaction products. CS, YS and ZS represent the corresponding activated species.

Campbell–Wojciechowski Mechanism

In the mechanism for cumene cracking proposed by Campbell and Wojciechowski (*9*) the reaction is initiated by the chemisorption of a cumene molecule on a single active site as suggested by Corrigan *et al.* (*10*) and Planck and Nace (*21*). This is followed by the removal of the alkyl group as a carbonium ion, releasing benzene to the gas phase. This mechanism, called the delta mechanism, is illustrated in Fig. 1 and includes the adsorption–desorption steps for the three major components as well as the reversible reaction of the chemisorbed cumene.

In a previous paper (*3*) a much more complex mechanism for cumene conversion was shown to apply in practice. The delta mechanism therefore represents only a subset of this general mechanism. However, the equations governing the kinetics of this subset of reactions are the same whether the whole mechanism or only this subset is being considered and can be used to interpret the kinetics of the dealkylation of cumene.

The species Y and Z in the mechanism can be identified by examining the reverse reaction. Workers who have studied the alkylation mechanism (*13, 15, 29, 30*) maintain that the reaction proceeds by a Rideal mechanism between an adsorbed propylene molecule and a molecule of benzene in the gas phase. Thus Y must be propylene while Z is benzene.

If it is assumed that the bond breaking step,

$$CS \underset{k-2}{\overset{k_2}{\rightleftharpoons}} YS + Z,$$

is the rate controlling step, then the rate of disappearance of cumene is written as

$$-r_c = k_2[CS] - k_{-2}[YS][Z], \quad (1)$$

where [CS], [YS], and [Z] represent, respectively, the concentration of adsorbed[4] cumene, adsorbed[4] propylene and gas phase benzene. Substituting for [CS] and [YS] in terms of Langmuir adsorption isotherms, accounting for volume expansion and for thermodynamic equilibrium, the resulting expression for the reaction rate was shown to be (*9*)

$$-r_c = \frac{k_2[S]K_1[C] - k_{-2}K_3[Y][S][Z]}{1 + K_1[C] + K_3[Y] + K_4[Z]}, \quad (2)$$

or in terms of conversion, x,

$$-r_c = \frac{k_2[S]K_1[C_0]}{x_e^2}\left(\frac{x_e^2 - x^2}{px^2 + qx + s}\right) \quad (3)$$

where

$$\begin{aligned} p &= K_3[C_0] + K_4[C_0] - K_1[C_0] + 1, \\ q &= K_3[C_0] + K_4[C_0] + 2, \\ s &= K_1[C_0] + 1 \end{aligned} \quad (4)$$

(note that $p = q - s$). In this expression x_e is the equilibrium conversion of cumene and can be calculated from thermodynamic data. $[C_0]$ is the initial concentration of cumene, and K_1, K_3, and K_4 are the adsorption[4] equilibrium constants for cumene, propylene and benzene. It was shown by Best and Wojciechowski (*6*) that the same type of expression is obtained if either adsorption of cumene or desorption of the products is rate controlling. The differences in such cases lie in the composition of the parameters, p, q, and s.

[4] We show below these constants must refer not to a simple adsorption process but to the formation of activated species.

On substituting Eq. (3) into the design equation for a plug flow reactor and accounting for catalyst decay with the Wojciechowski decay expression (*32*), the resulting expression becomes

$$Pbt_f(1 + Gt)^{-N} = -p'x + \frac{q'}{2}\ln\left(\frac{x_e^2}{x_e^2 - x^2}\right) + \frac{p'x_e^2 + s'}{2x_e} \times \ln\left(\frac{x_e - x}{x_e + x}\right), \quad (5)$$

where

$$p' = \frac{px_e^2}{k_2[S_0]K_1}, \qquad q' = \frac{qx_e^2}{k_2[S_0]K_1},$$

and

$$s' = \frac{sx_e^2}{k_2[S_0]K_1}$$

(note that $p' = q' - s'$).

Equation (5) is the final expression which relates instantaneous conversion (x) in a plug flow reactor to the instantaneous catalyst time on stream (t). The parameters of the model are: G, the aging parameter; N, the aging exponent; any two of p', s', q' combinations of the rate constants and the adsorption equilibrium constants for the major constituents of the reaction. However, since $q' = p' + s'$, and since it has been found that for cumene cracking on LaY zeolite $N = 1$, only three parameters need to be determined in practice, namely, G and two of p', s' or q'.

The variables in the model are instantaneous conversion x, instantaneous catalyst time on stream t, final catalyst time on stream t_f, and catalyst to feed weight ratio P, referred to as the cat/oil ratio. The average conversion after the catalyst has been on stream for a time t_f is determined from Eqs. (6) and (5) and it is this theoretical $\bar{x}$ that is compared to the

experimental cumene cracking data

$$\bar{x} = \frac{1}{t_f}\int_0^{t_f} x dt. \qquad (6)$$

The parameters p', q', and s' of the Campbell–Wojciechowski mechanism can also be used to study intraparticle diffusion limitations (*6*). Taking the ratios p'/s' and q'/s' the rate constant k_2 can be eliminated to yield

$$\frac{p'}{s'} = \frac{K_3[C_0] + K_4[C_0] - K_1[C_0] + 1}{K_1[C_0] + 1}, \qquad (7)$$

and

$$\frac{q'}{s'} = \frac{K_3[C_0] + K_4[C_0] + 2}{K_1[C_0] + 1}. \qquad (8)$$

As catalyst particle size increases, diffusion becomes more significant and $[C_0]$ approaches zero within the catalyst. Consequently,

$$\left.\begin{aligned} \frac{p'}{s'} &\to 1 \\ \frac{q'}{s'} &\to 2 \end{aligned}\right\} \text{ as } [C_0] \to 0 \text{ or as particle size} \to \infty. \qquad (9)$$

When diffusion becomes insignificant, $[C_0]$ within the catalyst becomes independent of particle size with the result that p'/s' and q'/s' approach the limit shown by Eq. (10).

$$\left.\begin{aligned} \frac{p'}{s'} &= \frac{K_3 + K_4 - K_1}{K_1} \\ \frac{q'}{s'} &= \frac{K_3 + K_4}{K_1} \end{aligned}\right\} \text{ as } [C_0] \to \infty. \qquad (10)$$

In our previous study of the reaction products of the cumene cracking reaction (*3*), it was shown that one of the correct methods of following the course of dealkylation reaction is to use a "corrected" benzene yield. At high temperatures there appears to be little reaction other than dealkylation to benzene and propylene; however, at lower temperatures the disproportionation of cumene in primary reactions becomes significant. In fact, at 360°C only 64% of the initially reacted cumene is converted by dealkylation. Consequently, total cumene disappearance is not a good measure of the extent of cracking. Neither is benzene yield unless one takes into account the benzene formed in the other primary reactions. Such corrected benzene yields are used as average conversion in this work to calculate the rate of cumene dealkylation.

EXPERIMENTAL RESULTS

A laboratory tubular reactor described in detail previously (*3*) was used in this study. The catalyst, a LaY zeolite, was also described in this earlier work. Experimental average conversion data were obtained with this apparatus using four ranges of particle sizes (100/140, 70/80, 40/45, and 20/25 mesh) and three reaction temperatures (500, 430, and 360°C) at cat/oil ratios ranging from 0.002 to 0.033 and catalyst times on stream up to 1000 sec. The cumene cracking model [Eqs. (5) and (6)] was fitted to these experimental data and least squares estimates of the three parameters G, p', and s' were determined. The fourth parameter, N, was in all cases found to be 1.0 as reported previously (*6, 9*). In keeping with earlier work (*9, 10, 21*) we have assumed the bond breaking step to be rate controlling.

The optimum values of G, p', and s' were determined using the minimum sum of squares of residuals as the criterion of fit. A residual is defined here as the difference between the experimental average conversion and that predicted theoretically using Eq. (6). The optimum estimates for the three parameters for all mesh sizes and reaction temperatures are listed in Table 2 along with the associated confidence limits. The theoretical curves determined using the least squares estimates of the

TABLE 2

A Summary of the Least Squares Estimates of the Model Parameters G, p' and s' Determined for the Cumeme Dealkylation Data[a]

Mesh size	Temp. (°C)	G (sec^{-1})	p' (sec)	s' (sec)
20/25	500	0.0108 ± 0.0009	0.00509 ± 0.0007	0.00274 ± 0.0002
	430	0.0201 ± 0.003	0.0142 ± 0.003	0.00238 ± 0.0003
	360	0.0850 ± 0.026	0.00689 ± 0.002	0.00250 ± 0.0005
40/45	500	0.0121 ± 0.001	0.00449 ± 0.0005	0.000770 ± 0.00008
	430	0.0231 ± 0.003	0.0110 ± 0.0005	0.00134 ± 0.0001
	360	0.0824 ± 0.01	0.00673 ± 0.001	0.00243 ± 0.0001
70/80	500	0.0143 ± 0.0004	0.00423 ± 0.0001	0.000303 ± 0.00003
	430	0.0256 ± 0.003	0.00906 ± 0.002	0.00101 ± 0.0002
	360	0.0795 ± 0.02	0.00669 ± 0.0006	0.00251 ± 0.0005
100/140	500	0.0144 ± 0.0009	0.00423 ± 0.0002	0.000303 ± 0.00003
	430	0.0259 ± 0.002	0.00901 ± 0.001	0.000902 ± 0.00007
	360	0.0806 ± 0.01	0.00654 ± 0.0004	0.00247 ± 0.0003

[a] Also shown in this table are the 95% confidence intervals associated with each parameter.

100/140 mesh parameters are shown in Fig. 2. Experimental data have been included in these figures.

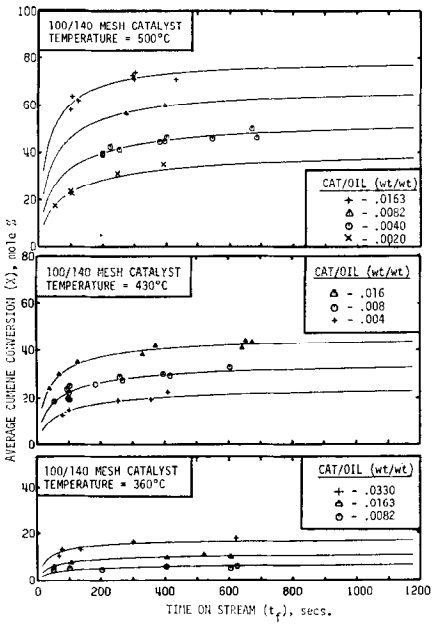

FIG. 2. Least squares fit of the cumene dealkylation data on the 100/140 mesh catalyst at the three reaction temperatures of 360, 430 and 500°C. (——) The theoretical cumulative conversion generated by Eqs. (5) and (6).

In Fig. 3 we show a selection of results obtained during the search for conditions independent of intraparticle diffusion limitations. In keeping with the recommendations of Best and Wojciechowski (*4*), a series of entire cat/oil curves was con-

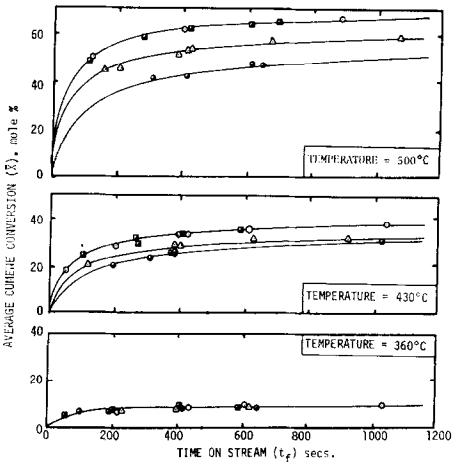

FIG. 3. Effect of particle size on total cumulative cumene conversion, for the three reaction temperatures of 500, 430 and 360°C at a cat/oil ratio of 0.0080. The symbols represent the following mesh sizes: (◑) 20/25; (△) 4045; (⬡) 70/80; and (◪) 100/140.

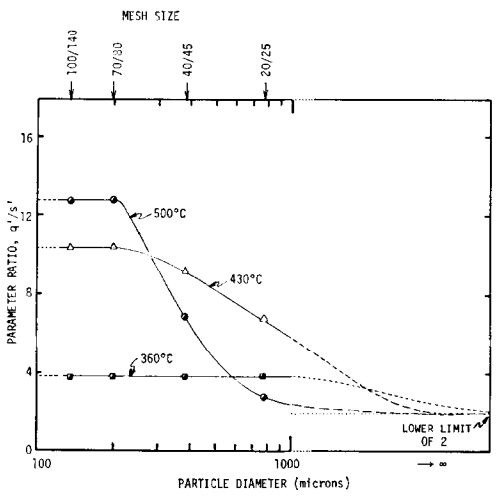

FIG. 4. Plot of the parameter ratio q'/s' against catalyst particle size for the three reaction temperatures studied.

structed for each mesh size of catalyst instead of the more usual approach of measuring conversion at a single space time for various catalyst particle sizes.

Figure 4 is a plot of the parameter ratio q'/s' against particle size for the three temperatures studied. As mentioned previously, this plot can also be used to evaluate intraparticle diffusion effects. The Arrhenius plots for the parameters s' and G are shown in Figs. 5 and 9 and they too show the influence of diffusion on the reaction.

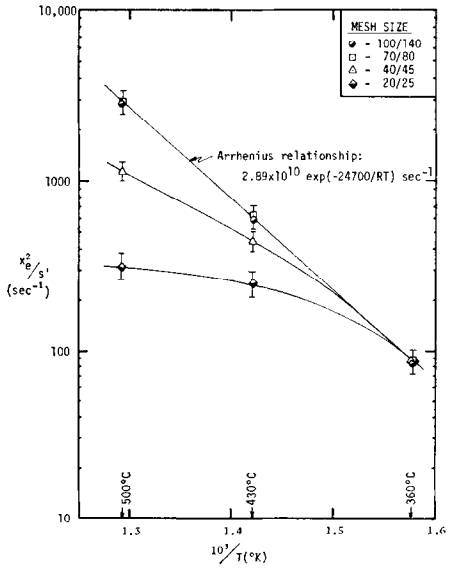

FIG. 5. Arrhenius plot of parameter x_e^2/s'.

Kinetic Parameters

The parameters of the cumene cracking model can be conveniently divided into two groups: the aging parameters (G and N) which are discussed in the next section and the kinetic parameters (p', q', and s') which are analyzed below. As a consequence of the assumption that the bond breaking step controls the rate of reaction, $q' = p' + s'$; hence only two of the kinetic parameters need to be considered in the discussion that follows. Because they are the least complex and therefore most amenable to analysis, q' and s' have been selected.

The parameter s' is used to establish the rate constant for the reaction. It is important therefore that the data used to determine s' be free of the effects of intraparticle diffusion in order to determine the intrinsic kinetics. As the LaY catalyst used in this study deactivates during the course of the reaction, the experimental approach outlined by Best and Wojciechowski (*4*) was used here to isolate the diffusion free region and the results have been reported in Fig. 3. From this figure it is evident that the 100/140 mesh catalyst is diffusion free at all reaction temperatures studied here. This is confirmed by an analysis of the parameter ratio q'/s' which, as noted earlier, also reflects the effects of intraparticle diffusion limitations.

The experimentally determined values of q'/s' are plotted in Fig. 4 for the three temperatures studied and it can be seen that the morphologies of these curves are consistent with theory as outlined above. At 500°C when the effects of intraparticle diffusion are most significant there is a rapid decrease in q'/s' toward 2 with in-

creasing particle size. However, q'/s' at 430°C decreases toward 2 less rapidly implying that the effects of intraparticle diffusion are less significant at this temperature. Furthermore, the fact that q'/s' does not approach this limit at 360°C over the range of particle sizes tested indicates that the reaction is sufficiently slow for diffusion effects not to be detected at that temperature. The broken portion of these curves, although hypothetical, have been included to illustrate the expected behavior of the family of curves.

In addition to the lower limit of 2 which is reached on a completely diffusion limited catalyst, the ratio will approach a second limit shown by Eq. (10) for $[C_0]$ approaching infinity. If $[C_0] = 1$ atm (which is the case in this study), the upper limit becomes

$$\frac{q'}{s'} = \frac{K_3 + K_4 + 2}{K_1 + 1}. \qquad (11)$$

As discussed previously, this limit will be reached when diffusion effects are insignificant. Such behavior can be observed in Fig. 4 where at 500°C this region of constant q'/s' is seen to occur only for catalyst smaller than 70/80 mesh. At 360°C, however, a constant q'/s' has been obtained for all mesh sizes studied.

Based on this analysis of q'/s' and the data in Fig. 3, it is obvious that data obtained on a catalyst smaller than 70/80 mesh will be independent of particle size and hence diffusion free for all temperatures studied here.

The rate constant for the reaction, k_2, can be extracted from the parameters s'. In its full form this parameter is written

$$\frac{x_e^2}{s'} = \frac{k_2[S_0]K_1}{1 + K_1[C_0]} \text{ (sec}^{-1}\text{)}, \qquad (12a)$$

or equivalently as

$$\frac{s'}{x_e^2} = \frac{[C_0]}{k_2[S_0]} + \frac{1}{k_2[S_0]K_1} \text{ (sec)}. \qquad (12b)$$

In these expressions, s'/x_e^2 is seen to be the sum of two exponentials which on an Arrhenius plot could produce two patterns—a straight line or a concave curve. However, when the experimental, diffusion free values of x_e^2/s' are plotted against inverse temperature as in Fig. 5, it is evident that the data lie on a straight line having the following temperature relationship:

$$\frac{x_e^2}{s'} = 2.89 \times 10^{10} \exp(-24.7 \times 10^3/RT) \text{ sec}^{-1}. \qquad (13)$$

Such a linear correlation can arise only if one of the following conditions holds: (a) both terms of Eq. (12b) have the same slope or (b) one term predominates. It is unlikely that both terms have the same slope since the first term of Eq. (12b), $[C_0]/k_2[S_0]$, has a slope of E_2/R while the second term, $1/k_2[S_0]K_1$, has a slope of $(E_2 - \Delta E_1)/R$. For the slopes to be comparable, $|\Delta E_1|$ would have to be much less than $|E_2|$ which is not expected to be the case. It appears to us that the alternative assumption is more likely, i.e., that one term in Eq. (12) is larger than the other. Two possibilities then exist: either $K_1[C_0] \ll 1$ or $K_1[C_0] \gg 1$.

In our previous work (*6*, *9*), it was established that under our conditions $K_1[C_0] \gg 1$ and as we have no reasons to reject this postulate, it is also accepted here. Notice that as a consequence of this assumption the rate equation for the loss of cumene shown as Eq. (2) reduces to

$$-r_c = \frac{k_2[S]K_1[C] - k_{-2}K_3[Y][S][Z]}{K_1[C] + K_3[Y] + K_4[Z]}. \qquad (14)$$

This equation becomes zero order at low conversions, which is in complete agreement with the findings of a number of workers who have studied the reaction (*16*, *22*, *23*). If, on the other hand, we had taken $K_1[C_0] \ll 1$ the rate equation would reduce to one that is first order in cumene at low

conversions, which is contrary to observations reported in the literature.

By assuming that $K_1[C_0] \gg 1$, Eq. (12a) reduces to

$$\frac{x_e^2}{s} = \frac{k_2[S_0]}{[C_0]}. \qquad (15)$$

Comparing this to Eq. (13) we see that

$$\frac{k_2[S_0]}{[C_0]} = 2.89 \times 10^{10} \exp\left\{\frac{-24.7 \times 10^3}{RT}\right\} \text{ sec}^{-1}.$$

Consequently, the rate constant for the reaction, $k_2[S_0]$, can easily be determined by multiplying through by $[C_0]$ to yield

$$k_2[S_0] = 1.17 \times 10^5 \exp\left\{\frac{-22.5 \times 10^3}{RT}\right\} \times \frac{\text{moles}}{(\text{g cat})(\text{sec})}.^5 \qquad (16)$$

The activation energy for the cracking reaction is therefore estimated to be 22.5 kcal/mole.

This fact leads to an immediate difficulty concerning the nature and energy requirements of the species immediately preceding the transition state for the reaction.

The endothermicity of the cumene cracking is known to be approximately 22 kcal/mole, whereas the activation energy of the activated species preceding the transition state is 22.5 kcal/mole. If we take the activated species to be an exothermically adsorbed entity we can not justify such a low activation energy for its reaction. If on the other hand we postulate endothermically formed carbonium ion which exists as a metastable activated species we can explain the energetics of this system.

An analysis of two possible energy diagrams for the reaction indicates which of the possibilities for cumene activation is more likely. The diagrams are shown in Fig. 6a and b. In both cases the diagrams have been constructed according to the condition that $K_1[C_0]$ is much greater than 1. They differ however in their representation of the energy required for the formation of the activated complex for cumene and propylene: in Fig. 6a this species is assumed to be formed endothermically while in Fig. 6b it is formed exothermically.

The labeling on these figures is consistent with the delta mechanism shown in Fig. 1, as well as the assumption that the bond

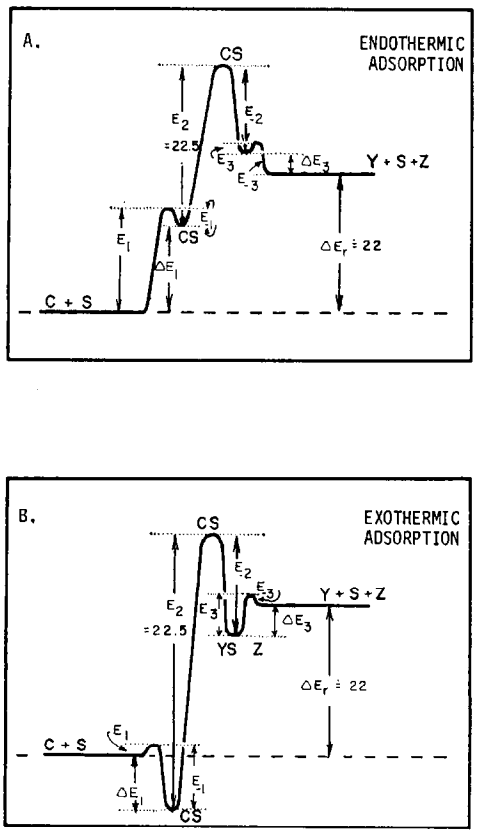

FIG. 6. Energy diagrams for cumene cracking. (A) Endothermic activation of chemisorbed intermediates; (B) exothermic activation.

[5] The initial pressure of cumene for this work was always 1 atm. Expressing $[C_0]$ in the units of g-moles/g cat, the ideal gas law was used. The values $[C_0]$ so calculated at different temperatures were then approximated by the equation $[C_0] = 4.05 \times 10^{-6} \exp(2.2/RT)$ g-moles/g cat.

breaking step controls the rate of reaction. "C + S" represents the energy level of a free cumene molecule and an active site, "CS" the energy level relative to "C + S" of an activated cumene molecule, "CS*" the relative energy level for the transition state, "YS + Z" the relative energy level of an activated propylene molecule and a free benzene molecule and finally "Y + S + Z," the energy level relative to "C + S" of a free propylene molecule, free benzene molecule and a free active site.

The total energy change for the reaction is denoted by ΔE_r which has been determined from thermodynamic analysis to be $\simeq$22 kcal/mole (*26*). E_{-2} represents the activation energy for the alkylation reaction

$$YS + Z \xrightarrow{k_{-2}} CS.$$

Literature values reported for E_{-2} at low temperatures are approximately 10 kcal/mole (*2, 19, 24*). E_2 represents the activation energy for the dealkylation reaction and its value has been determined here from the parameter s' to be 22.5 kcal/mole.

When all the energies are taken into account, an energy balance can be written as

$$\Delta E_r = (E_1 - E_{-1}) + (E_2 - E_{-2}) + (E_3 - E_{-3}). \quad (17)$$

Using the estimates of ΔE_r and E_2 cited above we obtain from this energy balance (which is applicable to either diagram)

$$22 = (E_1 - E_{-1}) + (22.5 - E_{-2}) + (E_3 - E_{-3}). \quad (18)$$

If exothermic estimates for ΔE_1 and ΔE_3 are used here together with the above value for E_{-2} then Eq. (18) becomes

$$\text{LHS} = 22.0,$$

$$\text{RHS} = 22.5 - 10.0 + (\Delta E_1 + \Delta E_3).$$

The left side of Eq. (18) is obviously not equal to the right side for any exothermic estimate of ΔE_1 and ΔE_3, such as those of Boreskova *et al.* (*8*) and others (*12*) for the physical adsorption of cumene or those for the physical adsorption of propylene (*8, 14*). However, if the activation of cumene and propylene is endothermic ($E_1 > E_{-1}$ and $E_3 > E_{-3}$) a balanced equation is possible. This clearly implies a semantic difficulty and an experimental problem in distinguishing between "activation" and "adsorption."

The picture of the kinetics of the cumene cracking reaction is now clear. A consideration of the overall energy balance and the parameter ratio q'/s' indicates that for this reaction the heats of formation of the reactive intermediates must be endothermic. The energy diagram in that case is shown in Fig. 6a.

Previous workers have failed to consider whether or not the value of activation energy they report is consistent with the energy requirements for the reaction. Consequently there has been no discussion of the possible existence of an endothermic activation step. From an energy point of view, we have shown why such activation is likely if a reaction activation energy of $\sim$23 kcal/mole is true for this case. From a chemical viewpoint, the endothermic activation step can be explained as a reaction in which a metastable carbonium ion intermediate is formed. Such carbonium ion formation can reasonably be assumed to be endothermic. Furthermore, that a metastable carbonium ion intermediate exists is made evident by data presented previously (*3*) where it was shown that this state undergoes bimolecular disproportionations with gas phase cumene molecules.

The preexponential factor for the various rate constants plotted in Fig. 7, determined from their intercept at $1/T = 0$, can be used as a measure of $[S_0]$, the concentration of active sites on the catalyst. As this intercept is larger for the LaY zeolite catalyst than for the cogelled silica-alumina catalyst used by Horton and Maatman (*16*), Maatman *et al.* (*17*) or

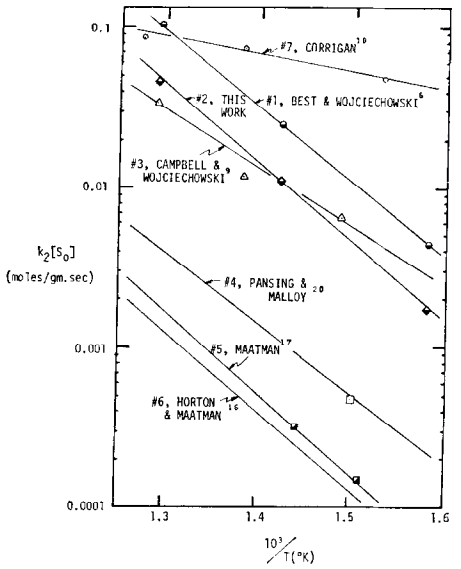

FIG. 7. A comparison of $k_2[S_0]$ determined in this work with those reported in the literature.

Pansing and Malloy (*20*), it appears that $[S_0]$ is greater for a LaY zeolite than for a cogelled silica–alumina catalyst, an interpretation which has been confirmed experimentally (*16*). It is impossible, however, to do anything but make a qualitative comparison with these cogelled catalysts. As noted earlier, these catalysts have been aged to some steady state level before any kinetic studies were performed, and unfortunately such pre-aging has been shown to yield an "observed" preexponential for $k_2[S_0]$ which is somewhat lower than the true value. This is not surprising of course since aging the catalyst reduces the number of unpoisoned sites available for reaction.

Effects of Intraparticle Diffusion on Kinetic Parameters

To this point, the discussion has concentrated on the intrinsic kinetics of the cracking reaction. However, using the data from the diffusion limited catalyst, a study can also be made of the effects of intraparticle diffusion. Such a study is straightforward if a non-aging catalyst is used but if the catalyst loses activity during the reaction the subsequent analysis becomes complicated.

In the usual situation in which a porous catalyst is used, significant mass transfer limitations within a catalyst will result in a concentration gradient throughout the particle. If the catalyst is non-aging, this gradient can be accounted for by multiplying the reaction rate constant by an effectiveness factor, η_r. Experimentally this effectiveness factor can be determined as

$$\eta_r = r_{dl}/r_{df}$$

where r_{dl} refers to the diffusion limited rate and r_{df} the diffusion free rate. If on the other hand the catalyst ages during the reaction the resulting rate expression will contain, in addition to the rate constant for reaction, a rate constant for decay which is contained in the aging parameter G. To account for diffusion, both constants must be modified by their respective effectiveness factors, η_r and η_d, which may be the same but usually are not. The consequences of this phenomenon were discussed in detail in an earlier paper (*4*).

When the appropriately modified rate constants for reaction and aging are used in the cumene cracking rate expression shown in Eq. (2), the resulting overall effectiveness factor shown in Eq. (19) is a complex function of time and conversion

$$\eta_{\text{overall}} = \left(\frac{p'x^2 + q'x + s}{(1 + Gt)^{-N}(x_e^2 - x^2)k_2[C_0]}\right)_{df} \times \left(\frac{(1 + G't)^{-N}(x_e^2 - x^2)k_2'[C_0]}{p'x^2 + q'x + s'}\right)_{dl}, \quad (19)$$

where $G' = \eta_d G$ and $k_2' = \eta_r k_2$ and subscripts *dl* and *df* represent diffusion limited and diffusion free rates, respectively.

In order to carry out a quantitative analysis it is better to look at initial rates of reaction where aging effects are insignificant. In this case, $x \to 0$, $t \to 0$ and Eq.

(19) reduces to

$$\eta_{\text{initial}} = s_{df}'/s_{di}'. \qquad (20)$$

Using the 100/140 mesh estimate of s' as the diffusion free value, the initial effectiveness factor has been determined according to this equation and the results for all reaction temperatures and mesh sizes are shown in the effectiveness factor plot in Fig. 8. These curves are typical of theoretical isothermal effectiveness factors in that η decreases more rapidly with increasing particle size at the highest temperature studied. At 360°C, η maintains a constant value of 1 which agrees with our previous statement that data obtained at this temperature are diffusion free for all sizes of catalyst studied.

The parameter x_e^2/s' is the initial rate of the cumene cracking reaction and the behavior of this parameter on an Arrhenius plot is shown as Fig. 5. The linear relationship demonstrated by the 100/140 mesh data in this figure represents the intrinsic rate, that is, the rate observed in the absence of diffusion when $\eta = 1$. The observed rate of reaction will be less than this intrinsic rate if intraparticle diffusion is significant; that is, when $\eta < 1$. Such a decrease in the reaction rate is illustrated in Fig. 5 by the 40/45 and 20/25 mesh data at temperatures above 360°C.

Aging Parameter Analysis

The two aging parameters N and G have been defined in an earlier paper by Wojciechowski (*31*) as

$$N = \frac{n}{m - 1}, \qquad (21)$$

and

$$G = (m - 1)k_d[\mathrm{P}], \qquad (22)$$

where

n number of sites used per cracking event

m number of sites lost per deactivating event

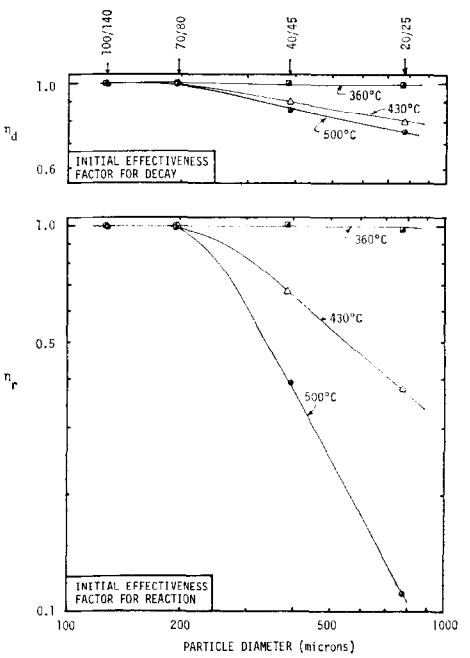

FIG. 8. Initial effectiveness factor for reaction and decay determined for the various temperatures and mesh sizes studied in this work.

k_d deactivation rate constant

[P] concentration of poisoning species P.

It is generally believed that cumene cracking results from the chemisorption of a cumene molecule on a single active site. Hence, n in the above definition of N is 1 and therefore, $m = 2$. This implies either a Hinshelwood deactivation mechanism in which two sites are lost per deactivating event, or a deactivation which proceeds by the adsorption of a poison on two sites. The fact that m is 2 under all the conditions studied supports the conclusion that diffusion has no effect on the mechanism of deactivation (*5*, *6*).

The second of the two aging parameters is G, and the effect of temperature on this parameter can be seen in the Arrhenius plot in Fig. 9. We recall that G contains a rate constant term k_d. If this rate constant behaves in a manner typical of elementary rate constants, then k_d should increase with increasing temperature. Since k_d is directly

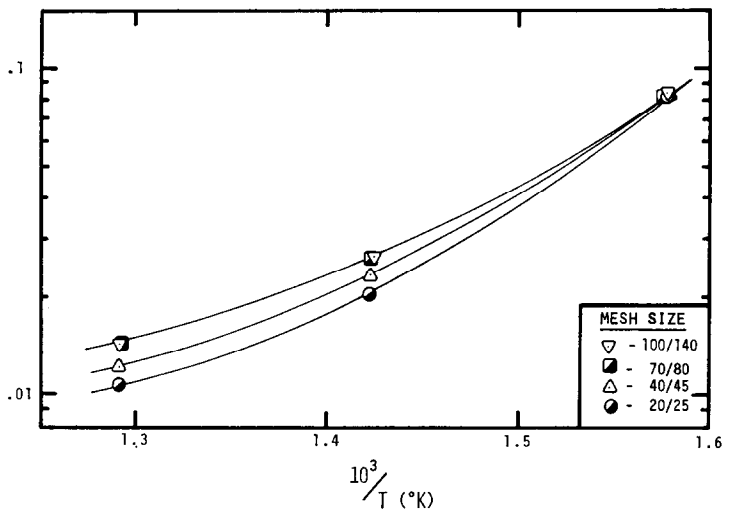

FIG. 9. Arrhenius plot of the aging parameter G for the four mesh sizes of catalyst studied in this work.

proportional to G, G should increase as well. However, as seen from Fig. 9, G in fact decreases with increasing temperature implying that the catalyst ages more rapidly at lower temperatures. This is the result of another temperature dependent term in the expression for G having a large negative exponential term. Further discussion of this is deferred to a subsequent paper in which an analysis of catalyst decay and its relationship to coke and minor product formation will be presented.

The effect of diffusion on G is also illustrated in Fig. 9. Here it can be seen that increasing diffusion limitation decreases G, hence decreases the rate of decay. This is consistent with our understanding of the diffusion process in that an increase in diffusion limitations is reflected by a decrease in the effective rate constant for deactivation and therefore a lower G.

If the diffusion free G is defined as $(m-1)k_d$ and the diffusion limited value defined as $\eta_d(m-1)k_d$, then the effectiveness factor for decay, η_d, is easily determined by the ratio G_{dl}/G_{df}. As before, the 100/140 mesh data is used to estimate the diffusion free value and the calculated η_d values for all mesh sizes and temperatures studied in this work are plotted in Fig. 8. From Fig. 8, it can be seen that $\eta_d < \eta_r$ for the same size catalyst at the same temperature. This implies that intraparticle diffusion affects the reaction rate to a greater extent than it does decay. The consequences of such unequal sensitivity of reaction and decay rates to diffusion limitation have been explored elsewhere (4).

CONCLUSION

We have shown that the three parameter Campbell–Wojciechowski model successfully correlates cumene dealkylation data on an aging catalyst over a wide range of temperatures, cat/oil ratios and diffusion limitation. From the parameters of this model, the intrinsic activation energy for the bond breaking step was determined to be 22.5 kcal/mole which was shown to be consistent with that reported by many other workers. If this value is accepted for the activation energy, an analysis of the parameter ratio q'/s' and of the energy surface for the reaction indicates that the adsorption of active species in this reaction is endothermic.

An analysis of the effects of intraparticle diffusion on the reaction indicates that

diffusion has no effect on the mechanism of catalyst decay. At the same time it is shown that an increase in diffusion limitations results in a greater decrease in the rate of conversion of cumene than in the rate of catalyst decay.

The above observations constitute experimental evidence in support of our theoretical treatment of the behavior of aging catalysts subject to diffusion limitations (*4*).

REFERENCES

1. Bassett, D. W., and Habgood, N. W., *J. Phys. Chem.* **64**, 796 (1960).
2. Becker, K. A., Karge, H. B., and Streubel, W. D., *J. Catal.* **28**, 403 (1973).
3. Best, D. A., and Wojciechowski, B. W., *J. Catal.* **47**, 11 (1977).
4. Best, D. W., and Wojciechowski, B. W., *Canad. J. Chem. Eng.* **54**, 197 (1976).
5. Best, D. A., Pachovsky, R. A., and Wojciechowski, B. W., *Canad. J. Chem. Eng.* **49**, 809 (1971).
6. Best, D. A., and Wojciechowski, B. W., *J. Catal.* **31**, 74 (1973).
7. Bezre, E. V., Romanovskii, B. V., Topchieva, K. V., and Thuoang, H. S., *Kinet. Katal.* **9**(4), 931 (1968).
8. Boreskova, E. G., Topchieva, K. V., and Piguzova, L. I., *Kinet. Katal.* **5**(5), 903 (1964).
9. Campbell, D. R., and Wojciechowski, B. W., *J. Catal.* **20**, 217 (1971).
10. Corrigan, T. E., Garver, J. C., Rase, H. F., and Kirk, R. S., *Chem. Eng. Progress*, **49**, 603 (1953).
11. Eberly, P. E., and Kimberlin, C. H., *Advan. Chem. Ser.*, **102**, 374 (1971).
12. Figueras, R. F., Renard, P., and deMourgues, L., *Method. Phys. Anal.* **4**(3), 298 (1968).
13. Germain, J. E., "Catalytic Conversion of Hydrocarbons" Academic Press, New York, 1969.
14. Golubev, V. S., Golubeva, E. E., Panchenkov, G. M., and Borisov, V. B., *Zh. Fiz. Khim.* **44**(12) 3106 (1970).
15. Haensel, V., *in* "Advances in Catalysis," (W. G. Frankenburg, V. I. Komarewsky and E. K. Rideal, Eds.), Vol. 3, p. 194. Academic Press, New York, 1951.
16. Horton, W. B., and Maatman, R. W., *J. Catal.* **3**, 113 (1964).
17. Maatman, R. W., Leenstra, D. L., Leenstra, A., Blankespoor, R. L., and Rubingh, D. H., *J. Catal.* **1**, 1 (1967).
18. Matsumoto, H., Yasui, K., and Morita, J., *J. Catal.* **12**, 84 (1968).
19. Panchenkow, G. M., and Kolesnikov, I. M., *Izv. Vysshikh Ucheb. Z., Neft GOZ* **5**, 55 (1959).
20. Pansing, W. F., and Malloy, J. B., *Ind. Eng. Chem., Process Des. Develop.* **4**, 181 (1965).
21. Planck, C. J., and Nace, D. M., *Ind. Eng. Chem.* **47**, 2374 (1955).
22. Prater, C. D., and Lago, R. M., *in* "Advances in Catalysis" (D. D. Eley, W. G. Frankenburg, V. I. Komarewsky and P. B. Weisz, Eds.), Vol. 8, p. 293. Academic Press, New York, 1956.
23. Richardson, J. T., *J. Catal.* **9**, 182 (1967).
24. Romanovskii, B. V., Bezre, E. V., and Topchieva, K. V., *Kinet. Katal.* **9**(5), 1111 (1968).
25. Romanovskii, B. V., Thuoang, K. S., Topchieva, K. V., and Piguzova, L. I., *Kinet. Katal.* **7**(5), 841 (1966).
26. Rossini, F. D., "Selected Values of Physical and Thermodynamic Properties of Hydrocarbon and Related Compounds," Carnegie Press, Pittsburgh, 1953.
27. Topchieva, K. V., Rosolovskaga, E. N., Zhavoronkov, M. N., Razanova, O. N., and Parmenova, N. S., *Dokl. Akad. Nauk SSSR.* **185**, 132 (1969).
28. Turkevich, J., and Ono, Y., *Advan. Chem. Ser.* **102**, 315 (1971).
29. Vento, P. B., *Advan. Chem. Ser.* **102**, 260 (1971).
30. Venuto, P. B., and Landis, P. S., *in* "Advances in Catalysis" (D. D. Eley, H. Pines and P. B. Weisz, Eds.), Vol. 18, p. 259. Academic Press, New York, 1968.
31. Wojciechowski, B. W., *Canad. J. Chem. Eng.* **46**, 48 (1968).
32. Wojciechowski, B. W., *Catal. Rev.* **9**(1), 79 (1974).